Hydrological Research Letters **18**(3), 79–86 (2024)
Published online in J-STAGE (www.jstage.jst.go.jp/browse/hrl). DOI: 10.3178/hrl.18.79

Thermal imaging survey for characterizing bedrock groundwater discharge: comparison between sedimentary and volcanic catchments

Kenta Iwasaki[1,2], Yu Nagasaka[3], Nobuo Ishiyama[3]* and Akiko Nagasaka[3]
[1]*Center for Forest Damage and Risk Management, Forestry and Forest Products Research Institute, Japan*
[2]*Doto Station, Forestry Research Institute, Hokkaido Research Organization, Japan*
[3]*Forestry Research Institute, Hokkaido Research Organization, Japan*

Abstract:

Groundwater discharge from bedrock varies depending on catchment conditions, particularly geology. In this study, we demonstrated the usefulness of a thermal infrared (TIR) camera for understanding the differences between two Mesozoic–Paleogene sedimentary catchments and two Quaternary volcanic catchments in Hokkaido, Japan. The TIR video survey effectively identified bedrock springs because of their low summer temperatures. Discharge rate of the cold bedrock springs was <0.005 L/s in the sedimentary catchments, whereas it exceeded 1 L/s in the volcanic catchments. However, the densities of bedrock springs were similar; they existed one point every 0.08–0.4 and 0.09–0.1 km in the sedimentary and volcanic catchments, respectively. Furthermore, differences in the concentrations of weathering-derived solutes from stream water were more than twice (up to 15 times) for some bedrock springs in the sedimentary catchments, whereas they were negligible for all springs in the volcanic catchments. These findings suggest that contributions from bedrock springs cannot be ignored even in sedimentary catchments with low bedrock permeability, especially when studying water chemistry. Spring water surveys using a TIR camera represents a fast and labor-saving method for characterizing bedrock groundwater discharge in catchments.

KEYWORDS thermal video; water temperature; groundwater spring; geology; bedrock permeability; water chemistry

INTRODUCTION

Groundwater that percolates into bedrock and discharges into downstream rivers has been reported worldwide (Fan, 2019; Somers and McKenzie, 2020) and is important for various watersheds. In catchments with considerable bedrock groundwater discharge, the structure of runoff models that rely on surface topography must be revised (Uchida *et al.*, 2021). Solute inputs from groundwater are also important for properly understanding biogeochemical processes and predicting land use and climate change impacts on stream chemistry (McGuire *et al.*, 2014; Peralta-Tapia *et al.*, 2015). Furthermore, groundwater discharge can affect the habitat of stream organisms (Ishiyama *et al.*, 2023; Sakai *et al.*, 2023; Sullivan *et al.*, 2021) and the functions of their ecosystems (Tolod *et al.*, 2022), because the temperature of groundwater is more stable than that of stream water. However, the quantity and quality of bedrock groundwater discharges vary depending on site conditions.

Catchment geology is an influential factor in bedrock groundwater dynamics (Pfister *et al.*, 2017; Richardson *et al.*, 2020; Tague and Grant, 2004). Comparisons of low-flow specific discharge throughout Japan have indicated that permeability is higher in Quaternary and Tertiary volcanic rocks and granite than in Tertiary and Paleo-Mesozoic sedimentary rocks (Musiake *et al.*, 1981; Shimizu, 1980). This does not mean that old sedimentary rocks are impermeable; bedrock flow paths have been reported even in Paleo-Mesozoic sedimentary catchments (Inaoka *et al.*, 2020; Onda *et al.*, 2004; Uchida *et al.*, 2002). The different geological permeabilities can cause contrasting patterns of bedrock groundwater discharge. A larger increase in specific discharge with drainage area (Iwasaki *et al.*, 2021) and smaller annual temperature fluctuations (Ishiyama *et al.*, 2023) of stream water suggest a greater amount of bedrock groundwater discharge in volcanic catchments compared to sedimentary catchments. However, it is not known how the water quality and spatial distribution of bedrock springs differ between these types of catchments.

The use of a thermal infrared (TIR) camera in summer or winter enables easy identification of springs, even if they are difficult to identify with the naked eye (Barclay *et al.*, 2022; Dugdale, 2016). The TIR imaging should be particularly effective for finding bedrock springs that discharge from a deep flow path. Iwasaki *et al.* (2023) developed a method using TIR video to conveniently map and sample groundwater discharge. The objective of this study was to demonstrate the usefulness of this method for geological comparison of the quantity, quality, and spatial distribution of bedrock springs. We compared the results of a TIR video-based spring water survey performed in summer between two Mesozoic–Paleogene sedimentary catchments and two Quaternary volcanic catchments in Hokkaido, Japan.

Correspondence to: Kenta Iwasaki, Center for Forest Damage and Risk Management, Forestry and Forest Products Research Institute, 1 Matsunosato, Tsukuba, Ibaraki 305-8687, Japan. E-mail: iwk@ffpri.affrc.go.jp
*Present address: Graduated School of Agriculture, Hokkaido University, Japan

Received 22 January, 2024
Accepted 23 May, 2024
Published online 30 August, 2024

METHODS

Site description

Observations were conducted at two sedimentary catchments (S-SE and S-NA) and a volcanic catchment (V-IR). The results at the S-SE and S-NA were compared with those from V-IR and another volcanic catchment underlain by Quaternary lava (V-FU; Site F in Iwasaki *et al.*, 2023). All sites are forested catchments within the Ishikari River basin in Hokkaido (Figure 1; Table SI). The S-SE and S-NA sites were included in the study area of Iwasaki *et al.* (2021), where the increasing contribution of deep groundwater with drainage area was determined using end-member mixing analysis (EMMA). The bedrock at these sites is mainly composed of Cretaceous or Eocene sandstone and mudstone (Figure 1). At the V-IR site, the Neogene sedimentary rock basement is covered by lava from the Irumukeppu Volcano, which is considered to have been active from the late Neogene to the early Quaternary. According to Kawano *et al.* (1956), the geology of the study area is classified as Irumukeppu agglomerate, the most abundant lava produced by this volcano.

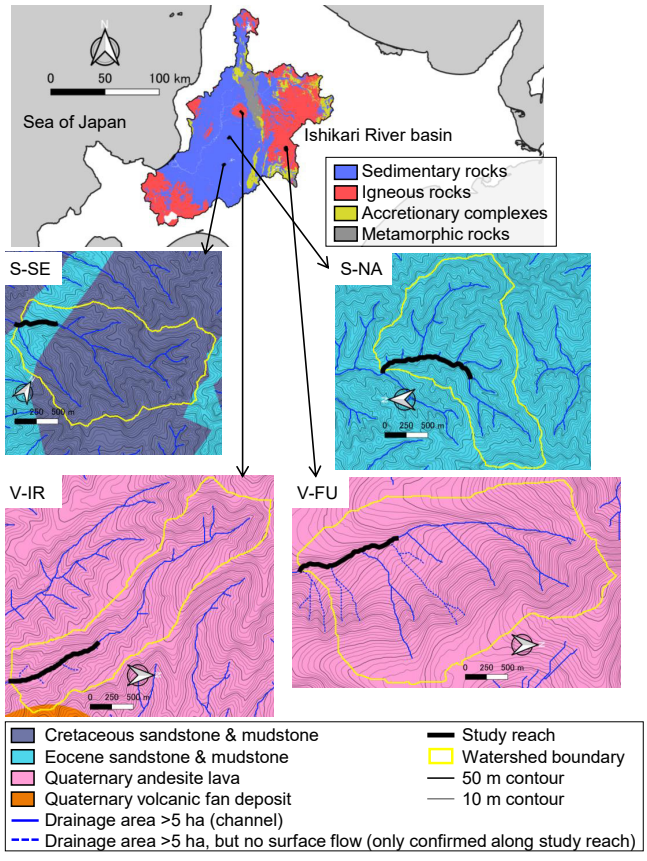

Figure 1. Maps of the study sites. The geological and topographic information was derived from the seamless Digital Geological Map of Japan (1:200,000) and the 10-m digital elevation models of the Geospatial Information Authority of Japan

Field survey, sampling, and chemical analysis

Survey dates and the meteorological conditions are summarized in Table SI. A field survey was performed on August 30 (12:25 p.m.–3:35 p.m.), August 31 (10:30 a.m.–3:03 p.m.), and September 1 (10:52 a.m.–3:12 p.m.), 2021 at S-SE, S-NA, and V-IR sites, respectively. The antecedent 7-day precipitation was small (≤ 7 mm) at all sites. Only at the S-SE site, a rain shower (21 mm) occurred during the survey, as recorded at a neighboring precipitation station (Miruto from the Water Information System of the Ministry of Land, Infrastructure and Transport, Japan; http://www1.river.go.jp/). A mainstream water sample collected upstream of the study reach before the rainfall had similar chemistry to one collected 170 m downstream after the rainfall (Figure S1). This suggests that the effect of the rainfall on stream chemistry was small, although this comparison does not account for the mixing of groundwater discharges between the two sampling points.

The detailed method of the survey using TIR video is described in Iwasaki *et al.* (2023), and a summary is presented here. We walked along the stream reach while recording images using a compact TIR camera (FLIR C3; FLIR Systems) connected to a tablet (Surface Go 2, Microsoft) with installed FLIR Tools+ software (FLIR Systems). The TIR images of the reach were monitored in real time and were recorded using FLIR Tools+. Location information was obtained at 1-s intervals using a handheld GPS (GPSmap 62sc; Garmin).

Water sampling and measurements of electrical conductivity (EC), water temperature, and discharge rates were performed at springs found by either TIR imaging or visual inspection, all tributaries with surface flow, and some points within the mainstream. Herein, springs were defined as surface waters with a drainage area of <5 ha, and larger surface inflows were considered tributaries. Note that no surface flow was found at some points at the volcanic sites despite the drainage area larger than 5 ha (dashed line in Figure 1), and we could not sample tributary water there. The samples were filtered through a GF/F filter with 0.63-μm pores in a laboratory and then refrigerated until analysis. Ion concentrations were measured using ion chromatography (Dionex ICS-1100; Thermo Fisher Scientific). EC and water temperature were measured using a portable meter (WM-32EP; DKK-TOA Corporation). Small spring flows were measured using the time required to fill a measuring cup. Discharge rates at the other sampling points were measured by multiplying their cross-sectional area by the flow velocity. The velocity was measured using a propeller flow velocity meter (CR-11; Miura-Rika Inc.) at 0.3-m intervals in mainstreams with channel widths >1.0 m. For springs and streams with narrower channels, the average velocity was measured by slowly moving the velocity meter across the channels over flat streambeds.

Mapping spring and stream temperatures

Spring and stream temperatures were mapped by post-processing the recorded TIR video in accordance with Iwasaki *et al.* (2023). First, time-series changes in the tentative minimum temperature of each frame (T_{TF}, °C) within a full screen were automatically obtained using FLIR Tools+. The minimum temperature was extracted because spring

and stream waters had lower surface temperatures than the land and above-water plants in many cases. These were tentative measurements because the T_{TF} was obtained using standard parameters (Table SII). The corrected minimum temperature of each frame (T_{CF}, °C) was then calculated using the following linear relationship:

$$T_{CF} = 0.84 \times T_{TF} + 3.4 \quad (1)$$

This equation was obtained from the relationship between the temperature measured by the portable meter and the T_{TF} from the TIR image from each sampling point (R^2 = 0.96; Figure S2). Data for springs with discharges <0.001 L/s were excluded from this analysis because the water temperature increased while a volume sufficient for the portable meter measurement was being collected. Equation 1 was similar to that obtained from two other sites by Iwasaki *et al.* (2023) (Figure S2).

The spatial distribution of T_{CF} was obtained by integrating its time-series changes into GPS tracks via time. Because two or three T_{CF} data were obtained per second, three consecutive data points were averaged when integrated with every second GPS data. For mapping, the minimum and median values of T_{CF} within a 5-m mesh grid was calculated using QGIS 3.22.7. We initially mapped the minimum values of T_{CF} in accordance with Iwasaki *et al.* (2023). Then, they were replaced with the median values for only the data with higher temperature than 15°C at the sedimentary sites because the stream had a higher temperature than ground or plants in some places (see RESULTS section). When using the minimum values, stream temperature was underestimated if there existed even one data point mistakenly extracted based on ground or plant surface temperatures. By using the median values, however, we could remove the influence of small amounts of such data on calculating stream temperature.

RESULTS

Discharge, temperature, and spatial distribution of springs at sedimentary sites

Cold springs with small discharge rates existed at the sedimentary sites. Eleven springs were found in the 0.5 km reach of the S-SE site. Six of these springs had water temperatures below 16°C, which was lower than those of the mainstream, land, and above-water plants (Figure S3). These "cold" springs discharged from bedrock fractures or under streambank rocks. The discharges of these springs were <0.005 L/s or too small to be measured (Figure 2 and Figure S3). Some spring discharges were gray and turbid and smelled of hydrogen sulfide (Figure S4). At the S-NA site, we found three springs with temperatures below 15°C within a 1.2 km reach. These cold springs also discharged from under the streambank rocks, and they had a discharge rate of <0.005 L/s (Figure 2 and Figure S5).

The locations of spring discharges with temperatures lower than the mainstream were identified using water temperature mapping (Figures 3a and 3b). In the original data, stream temperature fluctuated by 1°C–2°C at the S-SE site (Figure S6). This was because a surface temperature other than water was extracted as the minimum temperature in some places. Using the minimum value within a grid underestimated stream temperature in such places, although it can map as many cold springs as possible. Meanwhile, using the median value could obtain an almost homogeneous spatial distribution of stream temperature (distance upstream of about 70–180 m in Figure 3a). Therefore, mapping the median value for temperatures higher than 15°C (Figure 3) was effective in reducing both the errors of stream temperature and the oversights of cold springs.

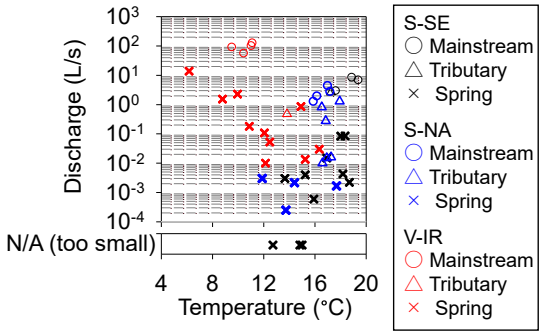

Figure 2. Relationship between temperature and discharge rate for stream and spring waters at the three sites: S-SE, S-NA, and V-IR

We could map cold springs scattered throughout the reach, which were not located within characteristic topographies (e.g. the outlet of a hollow with a drainage area >1 ha) (Figures 3a and 3b). The distribution of cold springs was one point every 0.08 km for the S-SE site and one point every 0.2–0.4 km for the S-NA site. The density for the S-NA site is presented as a range because seven points, except for one tributary, were mapped with temperatures below 15°C; thus, some springs may have been overlooked during the field survey.

Discharge, temperature, and spatial distribution of springs at volcanic sites

Unlike the sedimentary sites, a high discharge spring (13.9 L/s) gushed from rocks at the V-IR site, and it had the lowest temperature (6.2°C) among all springs at this site (Figure S7b; Movie S1). The 1.1-km reach in the V-IR site also had five other springs with discharges greater than those of the springs in the sedimentary sites (Figure 2). At the V-FU site, the spring discharge rates were not measured because the springs discharged with areal spread from streambanks. However, the average discharge per spring was calculated as 1.3 L/s during the baseflow period because a 1.3-km reach with 14 springs (13 were <9°C and one was 12°C) gained 18.8 L/s, excluding tributary inflows. Thus, both volcanic sites had greater spring discharge than the sedimentary sites.

Springs were mapped as being distributed every 0.09–0.1 km at locations without characteristic topography at both volcanic sites (Figures 3c and 3d). Spring and stream waters had lower surface temperatures than the ground and plants. This made it easy to find the springs in the field and extract only the water surface temperature if the water surface is included in the frame. However, some frames did not shoot the water surface; thus, a small amount of data had a higher temperature than the stream (Figures 3c and 3d). At the V-FU site, the data were regarded as abnormal

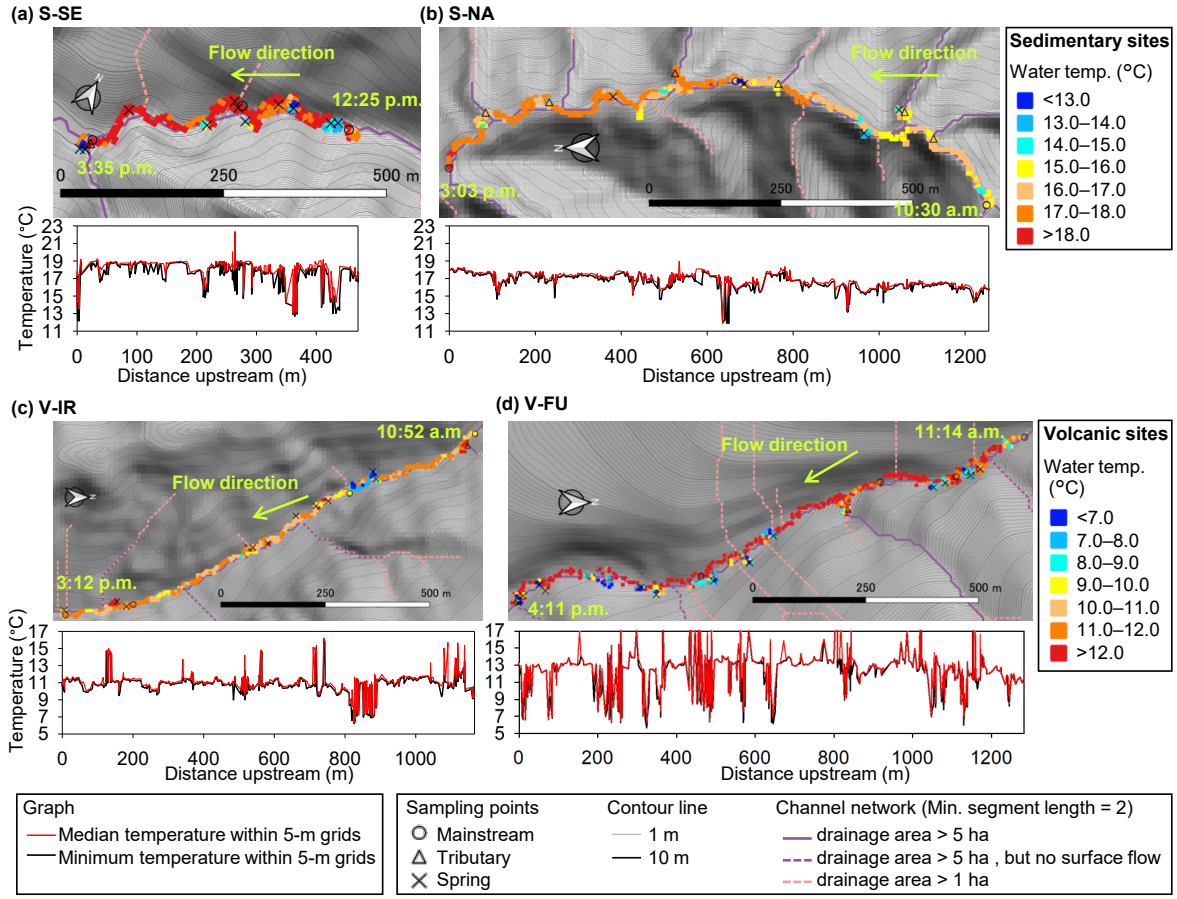

Figure 3. Water temperature maps generated from thermal infrared images. Data in the V-FU site are sourced from Iwasaki *et al.* (2023)

data without shooting water surface because almost no springs had a higher temperature than the stream (Figure 4). However, only two springs with large discharges were colder than the stream water at the V-IR site because of the low stream temperature (Figure 2). As a result, springs were mapped not only as lower temperature locations but also as higher temperature locations compared to stream water (Figure 3c). In such sites, it was difficult to distinguish whether the high temperature data indicate abnormal data or the existence of warm springs.

Characteristics of spring chemistry

Cold springs had highly variable concentrations of weathering-derived solutes (i.e. SO_4^{2-}, Na^+, Mg^{2+}, and Ca^{2+}) at the sedimentary sites (Figure 4). At the S-SE site, some cold springs (<16°C) had more than twice the solute concentration and EC of the stream water, and in particular, there was a 15-fold difference in SO_4^{2-} among them. At this site, the Cl^- concentrations of all the springs were about half those of the stream water. However, the stream Cl^- concentrations were much higher (400–500 µmol/L) than those at the other sites, suggesting the presence of springs with extremely high Cl^- concentrations upstream of the study reach. The S-NA site also had a <15°C springs with Na^+ and Ca^{2+} concentrations more than twice as high as the stream water, although the SO_4^{2-} concentrations were lower.

In contrast to the sedimentary sites, the concentrations of weathering-derived solutes were similar between streams and springs at the volcanic sites (Figure 4). However, even at the volcanic sites, NO_3^- concentrations were about twice as high in some springs compared to the stream water.

DISCUSSION

Characteristics of bedrock springs in sedimentary sites

Springs with colder temperatures than streams, small discharge rates of <0.005 L/s, and high concentrations of weathering-derived solutes existed every 0.08–0.4 km at the sedimentary sites. The chemical properties and on-site observation suggest that the cold springs were sourced from bedrock groundwater.

Cold springs had higher SO_4^{2-}, Na^+, Mg^{2+}, and Ca^{2+} concentrations than stream water, and springs with high Cl^- concentrations were suggested to exist upstream at the S-SE site (Figure 4). Two kilometers downstream from the study reach at this site, a mineral spring (i.e. spring with higher solute concentrations than the limits established by the Japanese Hot Spring Law) with a water temperature of 15.6°C and high concentrations of SO_4^{2-} (906 µmol/L), Na^+ (27,316 µmol/L), Cl^- (6,609 µmol/L), and Ca^{2+} (414 µmol/L)

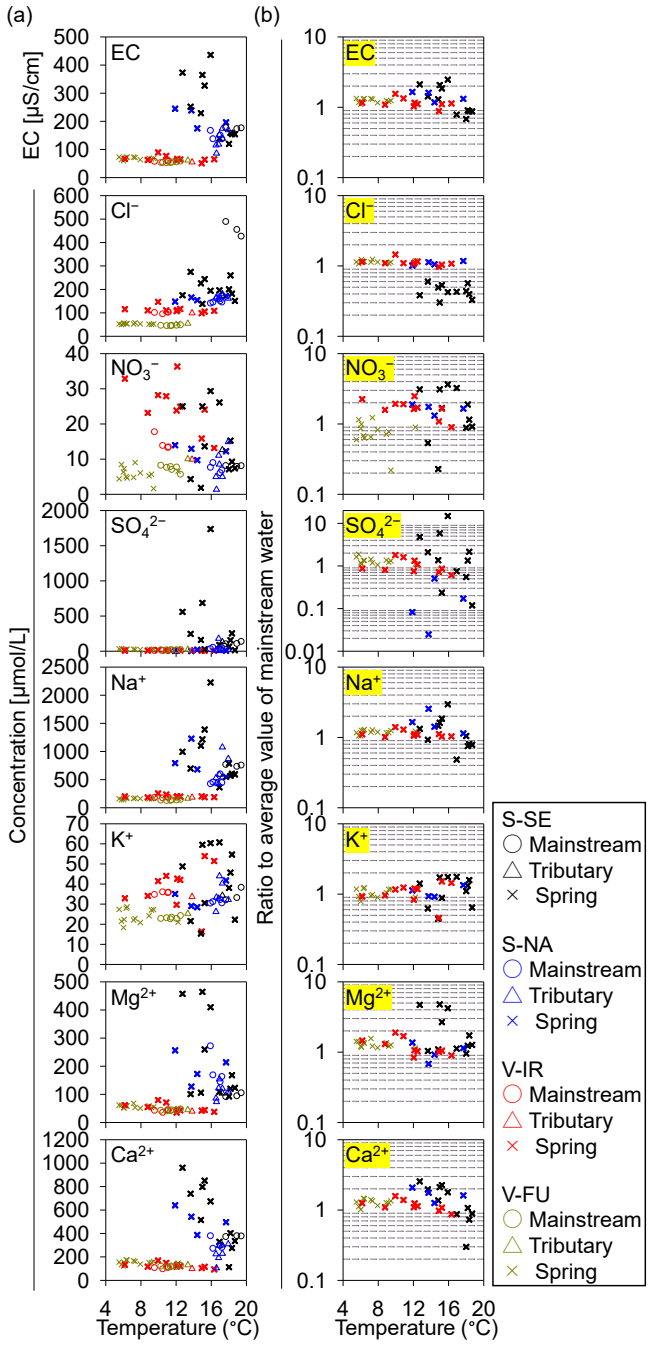

Figure 4. Relationships of water temperature to (a) EC and solute concentrations and (b) the ratio of spring water to average mainstream water in the corresponding catchment for each chemical component. Data in the V-FU site are sourced from Iwasaki *et al.* (2023)

discharges from Paleogene sedimentary rock (Matsunami *et al.*, 1994). A hot-spring inn that used this spring water after heating operated until 2008. In the surrounding area, many springs discharge from faults and fractures in Cretaceous sedimentary rocks (Matsuno *et al.*, 1964). The volume of these bedrock springs is often small and characterized by a faint hydrogen sulfide odor accompanied by a small amount of white sediment (Sasa *et al.*, 1964). Some springs had the same characteristics (Figure S4), and discharge from bedrock fractures was directly observed in a spring (Figure S3k). About 1 km downstream of the S-NA site, Matsunami *et al.* (1994) reported a cold (12.1°C) mineral spring from Paleogene sedimentary rocks with high Na^+ (12,832 µmol/L), Mg^{2+} (527 µmol/L), and Ca^{2+} (424 µmol/L) and low SO_4^{2-} (62 µmol/L) concentrations. This chemical property is similar to the cold springs at the S-NA site. These similarities with the bedrock groundwater reported near the site suggest that cold springs discharge from the Mesozoic–Paleogene sedimentary bedrock at the S-SE and S-NA sites.

The small discharge rates and extreme chemistry of bedrock springs are consistent with the previous knowledge on runoff mechanisms in sedimentary catchments. Water rapidly drained from the soil and shallow fractured bedrock generates headwater streams (Anderson *et al.*, 1997; Katsuyama *et al.*, 2008; Uchida *et al.*, 2002), and the remaining infiltrated water contributes downstream via the rock matrix and fractures within deep bedrock (Hale *et al.*, 2016; Kanazawa *et al.*, 2021) in catchments underlain by old sedimentary rock. Our results imply that narrow flow path within fractures caused the smaller volume and extreme chemistry of bedrock springs in the sedimentary catchments.

Characteristics of bedrock springs in volcanic sites

In the volcanic sites, springs discharged every 0.09–0.1 km and some of them had large discharge of >1 L/s. Although the springs had similar chemistry with stream water, they are also presumed to have originated from bedrock.

Generally, groundwater flow in lava and pyroclastic flow deposits supplies large amounts of spring water downstream at young volcanic mountains (Asai *et al.*, 2009; Hosono *et al.*, 2020; Tague and Grant, 2004). In this region, perennial stream flow seldom occurs in small catchments; thus, stream water itself is fed by springs from groundwater storage within highly permeable bedrock (Asai *et al.*, 2009; Fujimoto *et al.*, 2016; Zang *et al.*, 2023). If the catchment includes geological boundaries, springs from the lower layer would have different chemistry with streams from the upper layer. However, no geological boundaries existed within our study reach. In such a site condition, both the springs and stream water can be sourced from the same highly permeable bedrock layer (Iwasaki *et al.*, 2021). Thus, the springs and stream water probably had a similar flow path and did not differ in water chemistry.

Limitations of TIR video for bedrock spring survey

The TIR imaging was useful for identifying bedrock springs with cold summer temperatures. This method has an inherent limitation that it can be used only in summer or winter with considerable temperature differences between streams and springs. In addition, we noticed two new limitations by applying this method to the three sites.

First, a case existed where the assumption of lower water temperature in summer than the ground and plants did not hold. Sedimentary sites had higher stream temperatures than volcanic sites. In addition, the ground and plants were wetted by rain showers at the S-SE site. Because of this, water temperature could not be extracted as T_{CF} in some

places. Conducting survey on a sunny summer day to avoid this problem is preferable, especially in sedimentary catchments. However, if the problem arises, its impact can be reduced by mapping the median T_{CF} within the grid for warm water as we did in this study.

Secondly, detection of warmer springs than streams was another limitation. At the V-IR site, the distinction of warm springs from abnormal data without shooting the water surface was difficult using only thermal images. Simultaneous recording of visible images would be a solution to this problem.

Implications and future directions

The extreme bedrock spring chemistry indicates that studies of water chemistry cannot ignore their contributions. For instance, SO_4^{2-} concentrations in stream water have been used to assess the impact of sulfur oxides on forest ecosystems (e.g. Vuorenmaa *et al.*, 2018). In such cases, groundwater inflows with high SO_4^{2-} concentrations may lead to erroneous assessments. Sampling spring water with high solute concentrations is also important for EMMA studies to determine appropriate end members. At the volcanic sites, the difference in solute concentrations between stream and spring waters was small, but NO_3^- was an exception. Nagasaka and Nagasaka (2015), based on multipoint observations around the Irumukeppu Volcano, suggested that stream NO_3^- concentrations increased with the percentage of old *Abies sachalinensis* stands in the drainage area. Thus, spring NO_3^- concentrations may be affected by the surrounding vegetation. Considering the large variability in spring chemistry, sampling at many springs using TIR images would be helpful for the accurate interpretation of hydro-biogeochemical data.

The inference of bedrock groundwater dynamics from geological and/or topographic information remains difficult because it has been investigated in only small parts of large mountainous areas. The trends indicated by this study would be applicable to other sites to some extent because the greater volume of groundwater discharging from bedrock at the Quaternary volcanic sites compared to the old sedimentary sites (Figure 2) is consistent with previous geological comparisons of stream runoff (Iwasaki *et al.*, 2021; Musiake *et al.*, 1981; Shimizu, 1980) and water temperature (Ishiyama *et al.*, 2023). However, permeability varies according to many factors, for example, geological age, rock composition, topography, and faulting. Therefore, as Gomi (2018) noted, a preliminary survey before establishing an observation catchment is necessary to develop a robust research plan. Characterization of the groundwater dynamics of existing study sites would also be beneficial. For these purposes, our TIR-based spring survey would be useful because it is easy to conduct and can directly observe groundwater discharge from bedrock. It is then expected that the relationship between catchment conditions and bedrock groundwater dynamics can be typified as spring survey data accumulate.

CONCLUSION

The results of this TIR video survey showed that the density of bedrock springs was similar among our study sites regardless of geology, although the discharge per spring was smaller in Mesozoic–Paleogene sedimentary catchments than in the Quaternary volcanic catchments. Furthermore, in the sedimentary catchments, we found bedrock springs with more than twice (up to 15 times) higher concentrations of weathering-derived solutes than the stream water. These findings suggest that the contribution of bedrock springs along the reach cannot be ignored, even in less permeable geology, especially in studies on water chemistry. The TIR video survey used in the current study enabled the quick field detection and mapping of many bedrock springs with minimal effort. Therefore, this method is useful for characterizing bedrock groundwater dynamics in catchments containing various geological features.

ACKNOWLEDGMENTS

This study was supported by strategic research grants from the Hokkaido Research Organization, JSPS KAKENHI Grant Numbers JP18K18221, JP22H03796, and JP23H02241, and research funding for the Ishikari and Tokachi Rivers provided by the Ministry of Land, Infrastructure, Transport and Tourism of Japan.

SUPPLEMENTS

Figure S1. Mainstream water chemistry before and after rainfall at the S-SE site

Figure S2. Relationship between tentative water temperature from TIR images and water temperature measured using a portable meter

Figure S3. TIR and visible images of springs (a–k) and their location (h) at the S-SE site. The corrected water temperature T_{CF}, discharge rate, and shooting time are written above the images. Note that the legend on the TIR images is corrected to T_{CF}

Figure S4. Picture of springs with grayish turbidity at the S-SE site

Figure S5. TIR and visible images of springs (a–d) and their location (e) at the S-NA site. Values above the images and the legend are the same as in Figure S3

Figure S6. Original data of the corrected minimum temperature of each frame (T_{CF}). The interruption period of recording TIR videos during the survey is excluded from the calculation of elapsed time

Figure S7. TIR and visible images of springs (a–j) and their location (k) at the V-IR site. Values above the images and the legend are the same as in Figure S3

Table SI. Characteristics of the study sites and weather on the observation dates

Table SII. Parameters of the thermal infrared (TIR) camera

Movie S1. Spring with the greatest discharge at the V-IR site

REFERENCES

Anderson SP, Dietrich WE, Montgomery DR, Torres R, Conrad ME, Loague K. 1997. Subsurface flow paths in a steep,

unchanneled catchment. *Water Resources Research* **33**: 2637–2653. DOI: 10.1029/97WR02595.

Asai K, Satake H, Tsujimura M. 2009. Isotopic approach to understanding the groundwater flow system within an andesitic stratovolcano in a temperate humid region: case study of Ontake volcano, central Japan. *Hydrological Processes* **23**: 559–571. DOI: 10.1002/hyp.7185.

Barclay JR, Briggs MA, Moore EM, Starn JJ, Hanson AEH, Helton AM. 2022. Where groundwater seeps: evaluating modeled groundwater discharge patterns with thermal infrared surveys at the river-network scale. *Advances in Water Resources* **160**: 104108. DOI: 10.1016/j.advwatres.2021.104108.

Dugdale SJ. 2016. A practitioner's guide to thermal infrared remote sensing of rivers and streams: recent advances, precautions and considerations. *WIREs Water* **3**: 251–268. DOI: 10.1002/wat2.1135.

Fan Y. 2019. Are catchments leaky? *WIREs Water* **6**: e1386. DOI: 10.1002/wat2.1386.

Fujimoto M, Ohte N, Kawasaki M, Osaka K, Itoh M, Ohtsuka I, Itoh M. 2016. Influence of bedrock groundwater on streamflow characteristics in a volcanic catchment. *Hydrological Processes* **30**: 558–572. DOI: 10.1002/hyp.10558.

Gomi T. 2018. Monitoring in forest hydrology and its future. *Journal of Japan Society of Hydrology & Water Resources* **31**: 560–567 (in Japanese). DOI: 10.3178/jjshwr.31.560.

Hale VC, McDonnell JJ, Stewart MK, Solomon DK, Doolitte J, Ice GG, Pack RT. 2016. Effect of bedrock permeability on stream base flow mean transit time scaling relationships: 2. Process study of storage and release. *Water Resources Research* **52**: 1375–1397. DOI: 10.1002/2015WR017660.

Hosono T, Hossain S, Shimada J. 2020. Hydrobiogeochemical evolution along the regional groundwater flow systems in volcanic aquifers in Kumamoto, Japan. *Environmental Earth Sciences* **79**: 410. DOI: 10.1007/s12665-020-09155-4.

Inaoka J, Kosugi K, Masaoka N, Itokazu T, Nakamura K. 2020. Effects of geological structures on rainfall-runoff responses in headwater catchments in a sedimentary rock mountain. *Hydrological Processes* **34**: 5567–5579. DOI: 10.1002/hyp.13972.

Ishiyama N, Sueyoshi M, García Molinos J, Iwasaki K, Negishi JN, Koizumi I, Nagayama S, Nagasaka A, Nagasaka Y, Nakamura F. 2023. Underlying geology and climate interactively shape climate change refugia in mountain streams. *Ecological Monographs* **93**: e1566. DOI: 10.1002/ecm.1566.

Iwasaki K, Nagasaka Y, Nagasaka A. 2021. Geological effects on the scaling relationships of groundwater contributions in forested watersheds. *Water Resources Research* **57**: e2021WR029641. DOI: 10.1029/2021WR029641.

Iwasaki K, Fukushima K, Nagasaka Y, Ishiyama N, Sakai M, Nagasaka A. 2023. Real-time monitoring and postprocessing of thermal infrared video images for sampling and mapping groundwater discharge. *Water Resources Research* **59**: e2022WR033630. DOI: 10.1029/2022WR033630.

Kanazawa A, Masaoka N, Kosugi K, Katsuyama M, Nakaya H. 2021. Estimation of spring water recharge area in headwater catchments. *Journal of Japan Society of Hydrology & Water Resources* **34**: 100–114 (in Japanese). DOI: 10.3178/jjshwr.34.100.

Katsuyama M, Fukushima K, Tokuchi N. 2008. Comparison of rainfall-runoff characteristics in forested catchments underlain by granitic and sedimentary rock with various forest age. *Hydrological Research Letters* **2**: 14–17. DOI: 10.3178/hrl.2.14.

Kawano Y, Matsui K, Shimizu I. 1956. Explanatory text of the geological map of Japan, scale. 1: 50000, Utashinai, Hokkaido Development Agency, Sapporo, Japan, 38p (in Japanese with English summary).

Matsunami T, Yokoyama E, Okazaki N, Wakahama H. 1994. Spring water and groundwater of old coal mines in the Ishikari coal field, central Hokkaido. *Report of the Geological Survey of Hokkaido* **66**: 51–68 (in Japanese with English summary).

Matsuno K, Tanaka K, Mizuno A, Ishida M. 1964. Explanatory text of the geological map of Japan, scale. 1: 50000, Iwamizawa, Hokkaido Development Agency, Sapporo, Japan, 160p (in Japanese with English summary).

McGuire KJ, Torgersen CE, Likens GE, Buso DC, Lowe WH, Bailey SW. 2014. Network analysis reveals multiscale controls on streamwater chemistry. *Proceedings of the National Academy of Sciences of the United States of America* **111**: 7030–7035. DOI: 10.1073/pnas.1404820111.

Musiake K, Takahasi Y, Ando Y. 1981. Effects of basin geology on river-flow regime in mountainous areas of Japan. *Proceedings of the Japan Society of Civil Engineers* **1981**: 51–62 (in Japanese with English summary). DOI: 10.2208/jscej1969.1981.309_51.

Nagasaka Y, Nagasaka A. 2015. The effects of forest cover type and bedrock on the streamwater chemistry at the Irumukeppu mountains in central Hokkaido. *Boreal Forest Research* **63**: 59–62 (in Japanese). DOI: 10.24494/jfsh.63.0_59.

Onda Y, Tsujimura M, Tabuchi H. 2004. The role of subsurface water flow paths on hillslope hydrological processes, landslides and landform development in steep mountains of Japan. *Hydrological Processes* **18**: 637–650. DOI: 10.1002/hyp.1362.

Peralta-Tapia A, Sponseller RA, Ågren A, Tetzlaff D, Soulsby C, Laudon H. 2015. Scale-dependent groundwater contributions influence patterns of winter baseflow stream chemistry in boreal catchments. *Journal of Geophysical Research: Biogeosciences* **120**: 847–858. DOI: 10.1002/2014JG002878.

Pfister L, Martínez-Carreras N, Hissler C, Klaus J, Carrer GE, Stewart MK, McDonnell JJ. 2017. Bedrock geology controls on catchment storage, mixing, and release: a comparative analysis of 16 nested catchments. *Hydrological Processes* **31**: 1828–1845. DOI: 10.1002/hyp.11134.

Richardson CM, Zimmer MA, Fackrell JK, Paytan A. 2020. Geologic controls on source water drive baseflow generation and carbon geochemistry: evidence of nonstationary baseflow sources across multiple subwatersheds. *Water Resources Research* **56**: e2019WR026577. DOI: 10.1029/2019WR026577.

Sakai M, Hoshi G, Wakiya R. 2023. Ecosystem functions of a spring-fed tributary in providing foraging habitat and thermal refuge for juvenile masu salmon. *Ichthyology & Herpetology* **111**: 44–53. DOI: 10.1643/i2022050.

Sasa Y, Tanaka K, Hata M. 1964. Explanatory text of the geological map of Japan. scale 1: 50000, Yūbari, Hokkaido Development Agency, Sapporo, Japan, 174p (in Japanese with English summary).

Shimizu T. 1980. Relation between scanty runoff from mountainous watershed and geology, slope and vegetation. *Bulletin, Forestry & Forest Products Research Institute, Japan* **310**: 109–128 (in Japanese with English summary).

Somers LD, McKenzie JM. 2020. A review of groundwater in high mountain environments. *WIREs Water* **7**: e1475. DOI: 10.1002/wat2.1475.

Sullivan CJ, Vokoun JC, Helton AM, Briggs MA, Kurylyk BL. 2021. An ecohydrological typology for thermal refuges in streams and rivers. *Ecohydrology* **14**: e2295. DOI: 10.1002/eco.2295.

Tague C, Grant GE. 2004. A geological framework for interpreting the low-flow regimes of Cascade streams, Willamette River Basin, Oregon. *Water Resources Research* **40**: W04303. DOI: 10.1029/2003wr002629.

Tolod JR, Negishi JN, Ishiyama N, Alam MK, Rahman MATMT, Pongsivapai P, Gao Y, Sueyoshi M, Nakamura F. 2022. Catchment geology preconditions spatio-temporal heterogeneity of ecosystem functioning in forested headwater streams. *Hydrobiologia* **849**: 4307–4324. DOI: 10.1007/s10750-022-04992-9.

Uchida T, Kosugi K, Mizuyama T. 2002. Effects of pipe flow and bedrock groundwater on runoff generation in a steep headwater catchment in Ashiu, central Japan. *Water Resources Research* **38**: 24-1–24-14. DOI: 10.1029/2001WR000261.

Uchida T, Asano Y, Hiraoka M, Yokoo Y, Gomi T, Mizugaki S, Niwa S, Katsuyama M. 2021. Effects of spatial scales on runoff/sediment transport in mountain catchments (4): avenues for prediction improvement. *Journal of Japan Society of Hydrology & Water Resources* **34**: 192–204 (in Japanese with English summary). DOI: 10.3178/jjshwr.34.192.

Vuorenmaa J, Augustaitis A, Beudert B, Bochenek W, Clarke N, de Wit HA, Dirnböck T, Frey J, Hakola H, Kleemola S, Kobler J, Krám P, Lindroos AJ, Lundin L, Löfgren S, Marchetto A, Pecka T, Schulte-Bisping H, Skotak K, Srybny A, Szpikowski J, Ukonmaanaho L, Váňa M, Åkerblom S, Forsius M. 2018. Long-term changes (1990–2015) in the atmospheric deposition and runoff water chemistry of sulphate, inorganic nitrogen and acidity for forested catchments in Europe in relation to changes in emissions and hydrometeorological conditions. *Science of The Total Environment* **625**: 1129–1145. DOI: 10.1016/j.scitotenv.2017.12.245.

Zang C, Sugita M, Okita A, Bi S. 2023. Runoff characteristics of headwater catchments in a young volcanic region. *Journal of Hydrology* **620**: 129350. DOI: 10.1016/j.jhydrol.2023.129350.